

Determining Cardiac Fiber Orientation Using FSL and Registered Ultrasound/DTI volumes

James Dormer¹, Xulei Qin², Ming Shen³, Silun Wang⁴, Xiaodong Zhang⁴,
Rong Jiang³, Mary B. Wagner³, Baowei Fei^{2,5*}

¹ *Department of Nuclear and Radiological Engineering, George W. Woodruff School of Mechanical Engineering, Georgia Institute of Technology, Atlanta, GA*

² *Department of Radiology and Imaging Sciences, Emory University, Atlanta, GA*

³ *Department of Pediatrics, Emory University, Atlanta, GA*

⁴ *Yerkes National Primate Research Center, Emory University, Atlanta, GA*

⁵ *Department of Biomedical Engineering, Emory University and Georgia Institute of Technology, Atlanta, GA*

*E-Mail: bfei@emory.edu; Website: feilab.org

ABSTRACT

Accurate extraction of cardiac fiber orientation from diffusion tensor imaging is important for determining heart structure and function. However, the acquisition of magnetic resonance (MR) diffusion tensor images is costly and time consuming. By comparison, cardiac ultrasound imaging is rapid and relatively inexpensive, but it lacks the capability to directly measure fiber orientations. In order to create a detailed heart model from ultrasound data, a three-dimensional (3D) diffusion tensor imaging (DTI) with known fiber orientations can be registered to an ultrasound volume through a geometric mask. After registration, the cardiac orientations from the template DTI can be mapped to the heart using a deformable transformation field. This process depends heavily on accurate fiber orientation extraction from the DTI. In this study, we use the FMRIB Software Library (FSL) to determine cardiac fiber orientations in diffusion weighted images. For the registration between ultrasound and MRI volumes, we achieved an average Dice similarity coefficient (DSC) of $81.6 \pm 2.1\%$. For the estimation of fiber orientations from the proposed method, we achieved an acute angle error (AAE) of $22.7 \pm 3.1^\circ$ as compared to the direct measurements from DTI. This work provides a new approach to generate cardiac fiber orientation that may be used for many cardiac applications.

1. INTRODUCTION

Cardiac fiber orientation has been shown to have serious implications on electrophysiological and mechanical operations of hearts [1-4]. Knowledge of these orientations can supply a cardiologist with additional physiological data about current or potential cardiac diseases in a patient. In order to estimate the orientation of the cardiac fibers, magnetic resonance diffusion tensor imaging (MR-DTI) has been used for *in vivo* measurements [5, 6]. DTI measures the diffusion of water in a tissue under the effects of various magnetic gradients. The rate of water diffusion is highly dependent on the orientation of the fibers, with the prolate regions having the highest rate of diffusion and isotropic regions the lowest [7-9]. Due to the high cost in time and equipment required for MR imaging as well as restrictions in the population that can undergo an MRI scan, DTI is not always an option for patients. In contrast, the current ultrasound imaging technology is cost effective and easily tolerated by the population but does not currently have the capability of measuring fiber orientation. Unlike X-ray imaging or single-photon emission computed tomography, ultrasound imaging is non-ionizing, a favorable property for pediatric imaging where patients can be expected to live for many years and are thus more susceptible to stochastic effects from radiation.

Previously, our group has shown that fiber orientations from a DTI template could be mapped onto a cardiac ultrasound volume by deforming an MRI volume [10-13]. This involves creating binary masks for the ultrasound and MR volumes,

a time-intensive process. In this study, we propose to use the automatic segmentation in FMRIB Software Library (FSL) in order to reduce the time necessary for analysis, using FMRIB's Automated Segmentation Tool (FAST) to create masks in contrast to manual segmentation performed in Analyze or other data processing software. FAST uses a hidden Markov random field (HMRF), developed by Zhang *et al.* to enhance the automatic segmentation of noisy MR images [14]. Through the use of multiple iterations, FAST updates segmentation by placing constraints on a pixel by pixel basis depending on the value of neighboring pixels. Due to this automatic constraint system, local structure can be extracted from relatively noisy images without manual interaction. In addition, FMRIB's Diffusion Toolbox (FDT) was used to extract tensors from diffusion weighted images through probability density function modeling [15, 16]; and ultrasound images were denoised using the SUSAN (Smallest Univalued Segment Assimilating Nucleus) tool box in FSL.

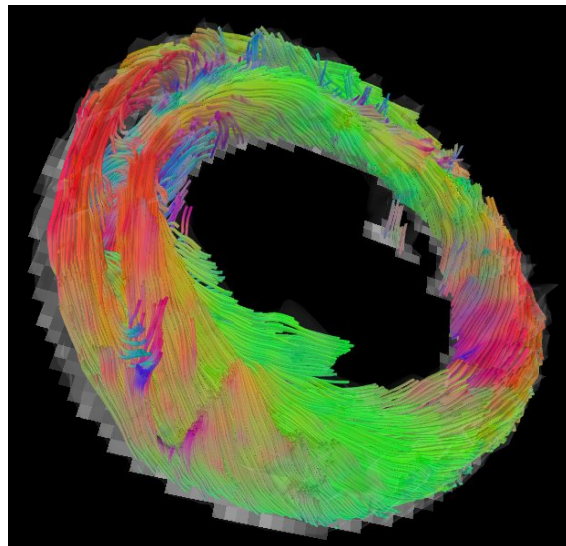


Fig. 1. Cardiac fibers reconstructed from magnetic resonance diffusion tensor imaging (MR-DTI). Red indicates a 90° orientation, while blue designates a -90° orientation.

2. METHODS

The basic workflow for the procedure is described in Fig. 2. The template geometry for the heart was determined from a T1 MRI and deformed onto an ultrasound mask from the target heart via affine and non-rigid transformations. Eigenvectors extracted from the template heart via diffusion tensor images were then mapped onto the registered US/MRI volumes. These fiber orientations were compared to the fiber orientation acquired from a DTI of the target heart.

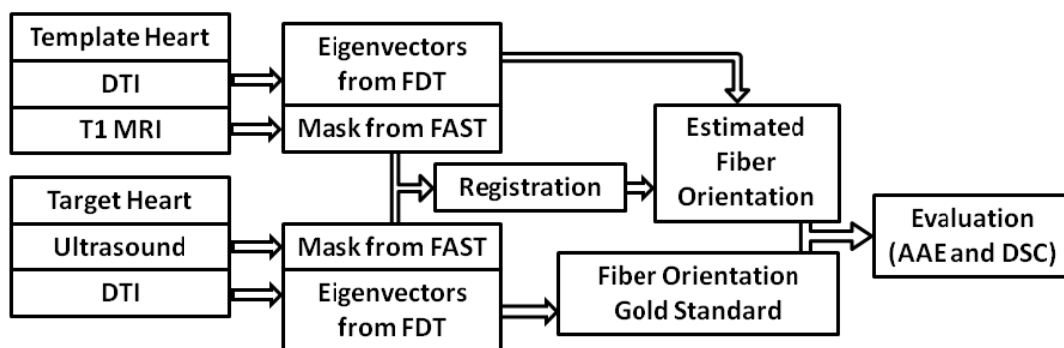


Fig. 2. Workflow for determining cardiac fiber orientation through the deformable registration of MR images and an ultrasound volume. FDT: FMRIB's Diffusion Toolbox. FAST: FMRIB's Automated Segmentation Tool.

2.1 Data acquisition

Healthy rat hearts were excised following IACUC approved methods as described previously [11, 17]. Briefly, each heart was perfused with cold 1xPBS solution to remove blood from the chambers. Each heart was then fixed using a solution of 4% phosphate buffered paraformaldehyde (PFA). After 14 hours, the hearts were rinsed with 1xPBS to remove PFA residue and embedded into 2% agar to create a cylindrical phantom.

Ultrasound images were acquired using a Vevo 2100 ultrasound system (FUJIFILM VisualSonics, Inc., Toronto, Canada) with a 30 MHz transducer and the B-mode method. A slice thickness of 0.2 mm was used with the short-axis view to image the heart from apex to base, encompassing the entire heart volume. A 7 T Biospec MRI system (Bruker Corp, MA, USA) with an RF coil of 25 mm diameter was used to acquire MR images. The pixel size was 0.234 mm^2 with 30 directions using a diffusion weighted spin echo imaging sequence. Anatomical information was provided by a T1 MRI at a resolution of $0.078 \times 0.078 \times 0.156 \text{ mm}^3$. The total scan time of the DTI for each heart was 36 hours.

2.2 Mask creation

Ultrasound volumes were first loaded into FSL's SUSAN (Smallest Univalve Segment Assimilating Nucleus) tool box developed from the algorithm created by Smith and Brady [18]. SUSAN uses a local mask to enhance detected features in an image by comparing intensity across the mask to that of the mask nucleus. The regions inside the mask which contain intensities similar to that of the nucleus provide feature information and allowing speckle reduction without the loss of structures. Results from SUSAN for one rat heart are shown in Fig. 3, which used a local mask of $10 \times 10 \times 10$ pixels as the region of interest for smoothing. The T1 MR image and despeckled ultrasound image were then loaded into the FMRIB's Automatic Segmentation Tool (FAST) to produce binary masks (Fig. 4 A2). The use of hidden Markov random fields allows FAST to identify structures based on neighboring pixel information in order to preserve image information even in noisy environments [14]. For the T1 images, the Markov random field (MRF) value was set to 0.1 with a bias field smoothing of 20 pixels for 4 iterations. Ultrasound images used an MRF of 0.25 with a bias field smoothing of 30 pixels for a single iteration. Three classes were used for the segmentation of both sets of volumes. After generating the output images, each was compared visually and the best for each individual volume was selected for further use.

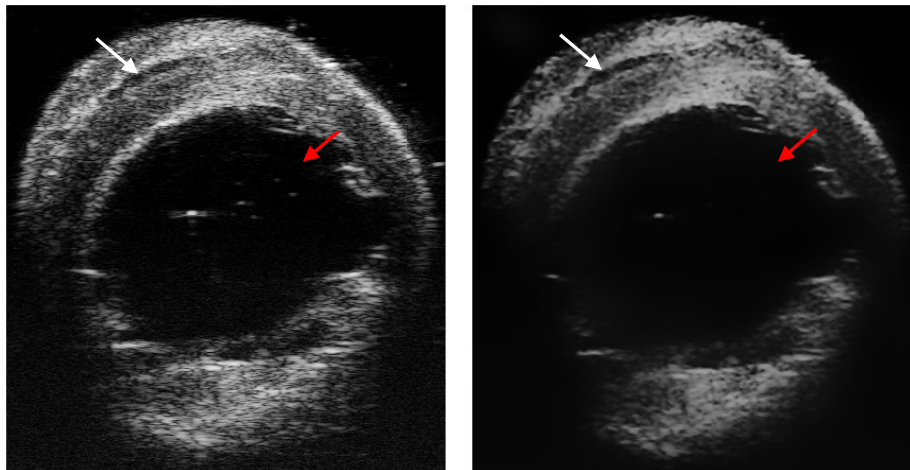


Fig. 3. Example of a rat heart ultrasound image with visible left ventricle (red arrow) and right ventricle (white arrow) before and after denoising in SUSAN. Left: Original ultrasound image. Right: Noise reduction using the nearest 10 pixels with an appropriate brightness threshold.

2.3 Fiber orientation estimation

The DTI volumes were first registered to the corresponding T1 volume. The registered DTI volume was then loaded into the FMRI's Diffusion Tool's DTIFIT package. The T1 binary mask created in FAST was used to identify the region of interest. In addition, the magnetic gradient directions and b values used to acquire the DTI were inserted into DTIFIT in order to extract the eigenvectors. FDT fits the measured diffusion within a voxel to a tensor model, enabling the calculation of a probability density function for the primary direction of diffusion even in the presence of noise or segmented signals. The primary direction is the first eigenvector and is thus assumed to be the orientation of the fiber. After acquiring the fiber orientations, the MR and ultrasound masks were loaded into Analyze (AnalyzeDirect Inc., Overland Park, USA) to perform a manual affine registration between the ultrasound and MR volumes. The rigidly registered template heart (T1 MR) mask was then registered using the log-Demons deformable registration [19] to the ultrasound mask of the target heart. The fiber orientations in each voxel of the template heart are then deformed onto the ultrasound image by using the preservation of principal direction (PPD) approach [20]. A DTI of the target heart enables a validation of the estimated cardiac fiber orientations after deformation.

2.4 Evaluation

Performance of the proposed method was evaluated by applying the Dice similarity coefficient [10, 11] to determine the similarity between ultrasound and MR image volumes, where R is the target volume and T is the deformed template volume. A DSC value of 100% indicates perfect overlap of the volumes.

$$DSC(R, T) = \frac{2Volum(R \cap T)}{Volum(R) + Volum(T)} \quad (1)$$

The accuracy of the fiber orientation estimation was evaluated using the acute angle error measured by inverting the 3D dot product between the ground truth (v_1) and the estimated fiber orientation (v_2) for each voxel in order to determine the separation in the orientation angle [20, 21]. An AAE of 0° signifies complete overlap of fibers between the estimated orientations and the ground truth.

$$AAE = \cos^{-1} \frac{|\bar{v}_1 \cdot \bar{v}_2|}{\|\bar{v}_1\| \|\bar{v}_2\|} \quad (2)$$

3. RESULTS

This method was evaluated on cardiac ultrasound and MR volumes from 5 different rats. Two rat hearts were chosen to use as templates. The results were quantified by a DSC and AAE (Table I). The average DSC and AAE were 81.6±2.1% and 22.7±3.1 degrees, respectively.

Typical results from the described procedure are displayed in Fig. 4. Binary segmentation results are shown in Fig. 4 A2 for T1 volumes and in Fig. 4 B2 for despeckled ultrasound volumes. After segmentation, these volumes were registered with the log-Demons approach, with the results shown in Fig. 5. The registration map produced by log-Demons was then applied to the fiber orientations from the DTI to estimate the fiber orientations of the heart imaged with ultrasound. These fiber orientations are exhibited in Fig. 4 C1-C2 with a comparison of deformed the fiber orientations to the actual orientations shown in Fig. 4 C3.

Table I: Quantitative results for fiber orientation extraction.

| Template | Target | DSC | AAE (degree) |
|----------|--------|-------|--------------|
| Rat 1 | Rat 2 | 84.6% | 24.2 |
| Rat 1 | Rat 3 | 79.3% | 17.1 |
| Rat 1 | Rat 4 | 80.6% | 26.7 |
| Rat 1 | Rat 5 | 82.8% | 19.8 |
| Rat 2 | Rat 1 | 82.7% | 24.5 |
| Rat 2 | Rat 3 | 79.0% | 22.3 |
| Rat 2 | Rat 4 | 80.2% | 25.0 |
| Rat 2 | Rat 5 | 83.3% | 21.8 |

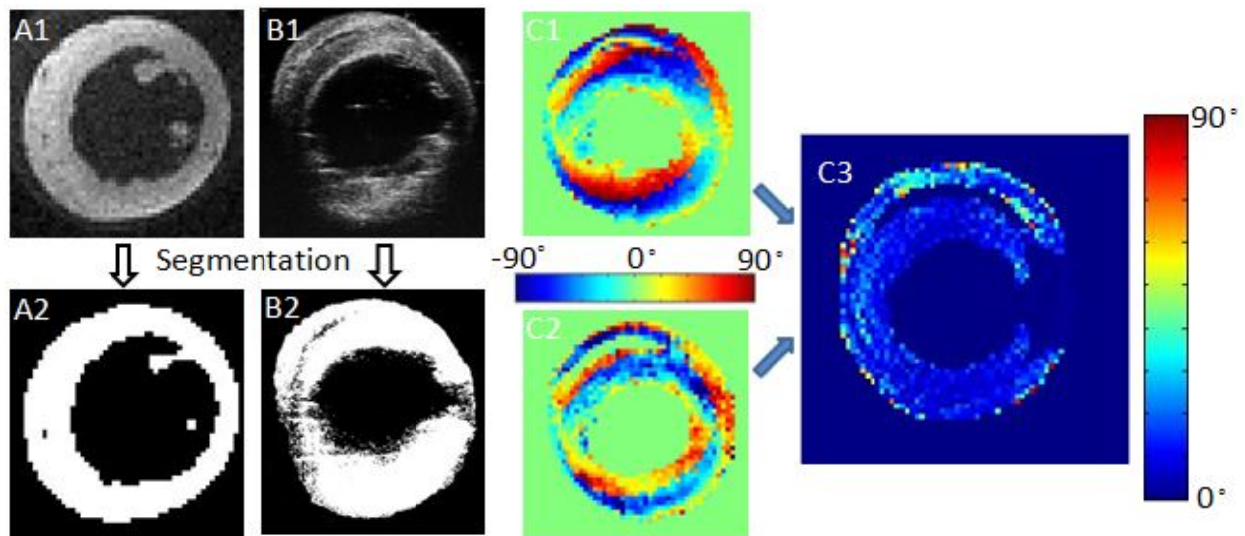


Fig. 4. Results from the automatic segmentation and subsequent fiber orientation calculations. (A1-A2) MR-DTI and the corresponding mask. (B1-B2) Ultrasound image and the corresponding mask. (C1) Estimated fiber orientations from 3D ultrasound using the proposed method. (C2) Actual fiber orientations from DTI. (C3) Error between actual and estimated fiber orientations.

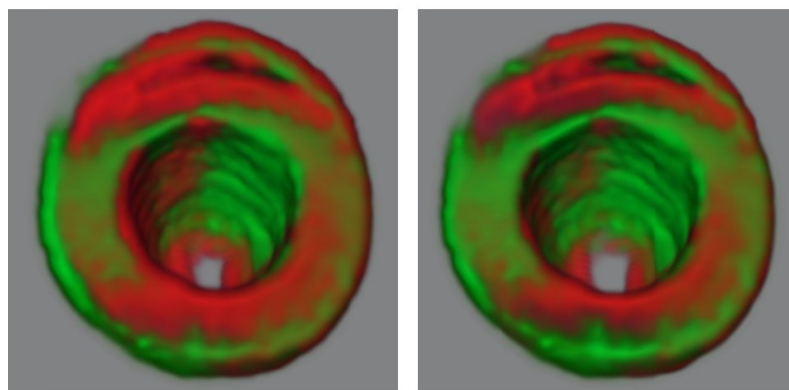


Fig. 5. Left and right ventricle cut-away of 3D results from the non-rigid deformation of rat hearts. Green: Ultrasound image. Red: T1 MR image. Left: Overlay of the ultrasound and original MR volumes. Right: Overlay of the ultrasound and deformed MR volumes.

4. CONCLUSIONS

We proposed and developed an approach for estimating cardiac fiber orientation from 3D ultrasound volumes by using an MR-DTI template. We have shown that FSL can successfully be applied to cardiac diffusion weighted MR images and ultrasound images for segmentation and cardiac fiber orientation determination using FAST and DTIFIT. Ultrasound images can be despeckled using SUSAN in FSL. The fiber orientation estimation method can provide a tool for many cardiac applications.

ACKNOWLEDGEMENTS

This work was partially supported by NIH grants (CA176684 and CA156775).

REFERENCES

- [1] H. Lombaert, J. M. Peyrat, P. Croisille, S. Rapacchi, L. Fanton, F. Cheriet, P. Clarysse, I. Magnin, H. Delingette, and N. Ayache, "Human atlas of the cardiac fiber architecture: study on a healthy population," *IEEE Trans Med Imaging*, 31(7), 1436-47 (2012).
- [2] M. Sermesant, R. Chabiniok, P. Chinchapatnam, T. Mansi, F. Billet, P. Moireau, J. M. Peyrat, K. Wong, J. Relan, K. Rhode, M. Ginks, P. Lambiase, H. Delingette, M. Sorine, C. A. Rinaldi, D. Chapelle, R. Razavi, and N. Ayache, "Patient-specific electromechanical models of the heart for the prediction of pacing acute effects in CRT: a preliminary clinical validation," *Med Image Anal*, 16(1), 201-15 (2012).
- [3] F. Vadakkumpadan, H. Arevalo, C. Ceritoglu, M. Miller, and N. Trayanova, "Image-based estimation of ventricular fiber orientations for personalized modeling of cardiac electrophysiology," *IEEE Trans Med Imaging*, 31(5), 1051-60 (2012).
- [4] P. M. Boyle, J. C. Williams, C. M. Ambrosi, E. Entcheva, and N. A. Trayanova, "A comprehensive multiscale framework for simulating optogenetics in the heart," *Nature Communications*, 4, (2013).
- [5] D. F. Scollan, A. Holmes, R. Winslow, and J. Forder, "Histological validation of myocardial microstructure obtained from diffusion tensor magnetic resonance imaging," *American Journal of Physiology-Heart and Circulatory Physiology*, 275(6), H2308-H2318 (1998).
- [6] F. Vadakkumpadan, H. Arevalo, C. Ceritoglu, M. Miller, and N. Trayanova, "Image-based estimation of ventricular fiber orientations for patient-specific simulations," *Conf Proc IEEE Eng Med Biol Soc*, 1672-5 (2011).
- [7] L. Geerts-Ossevoort, P. Bovendeerd, F. Prinzen, T. Arts, and K. Nicolay, "Myofiber orientation in the normal and infarcted heart, assessed with MR-diffusion tensor imaging," *Computers in Cardiology*, 621-624(2001).
- [8] L. Geerts, P. Bovendeerd, K. Nicolay, and T. Arts, "Characterization of the normal cardiac myofiber field in goat measured with MR-diffusion tensor imaging," *American Journal of Physiology-Heart and Circulatory Physiology*, 283(1), H139-H145 (2002).
- [9] M. T. Wu, W. Y. I. Tseng, M. Y. M. Su, C. P. Liu, K. R. Chiou, V. J. Wedeen, T. G. Reese, and C. F. Yang, "Diffusion tensor magnetic resonance imaging mapping the fiber architecture remodeling in human myocardium after infarction - Correlation with viability and wall motion," *Circulation*, 114(10), 1036-1045 (2006).
- [10] X. L. Qin, and B. W. Fei, "DTI template-based estimation of cardiac fiber orientations from 3D ultrasound," *Medical Physics*, 42(6), 2915-2924 (2015).
- [11] X. Qin, S. Wang, M. Shen, X. Zhang, M. B. Wagner, and B. Fei, "Mapping cardiac fiber orientations from high resolution DTI to high frequency 3D ultrasound," *SPIE Medical Imaging 2014: Image-Guided Procedures, Robotic Interventions, and Modeling*, 9036, (2014).
- [12] X. Qin, and B. Fei, "Measuring myofiber orientations from high-frequency ultrasound images using multiscale decompositions," *Phys Med Biol*, 59(14), 3907-3924 (2014).
- [13] X. Qin, Z. Cong, R. Jiang, M. Shen, M. B. Wagner, P. Kirshbom, and B. Fei, "Extracting cardiac myofiber orientations from high frequency ultrasound images". *Proc. SPIE* 8675, 867507-8.

- [14] Y. Y. Zhang, M. Brady, and S. Smith, "Segmentation of brain MR images through a hidden Markov random field model and the expectation-maximization algorithm," *Ieee Transactions on Medical Imaging*, 20(1), 45-57 (2001).
- [15] T. E. J. Behrens, M. W. Woolrich, M. Jenkinson, H. Johansen-Berg, R. G. Nunes, S. Clare, P. M. Matthews, J. M. Brady, and S. M. Smith, "Characterization and propagation of uncertainty in diffusion-weighted MR imaging," *Magnetic Resonance in Medicine*, 50(5), 1077-1088 (2003).
- [16] S. Jbabdi, S. N. Sotiropoulos, A. M. Savio, M. Grana, and T. E. J. Behrens, "Model-based analysis of multishell diffusion MR data for tractography: How to get over fitting problems," *Magnetic Resonance in Medicine*, 68(6), 1846-1855 (2012).
- [17] X. L. Qin, S. L. Wang, M. Shen, X. D. Zhang, S. Lerakis, M. B. Wagner, and B. W. Fei, "3D in vivo imaging of rat hearts by high frequency ultrasound and its application in myofiber orientation wrapping," *Medical Imaging 2015: Ultrasonic Imaging and Tomography*, 9419, (2015).
- [18] S. M. Smith, and J. M. Brady, "SUSAN - A new approach to low level image processing," *International Journal of Computer Vision*, 23(1), 45-78 (1997).
- [19] T. Vercauteren, X. Pennec, A. Perchant, and N. Ayache, "Symmetric Log-Domain Diffeomorphic Registration: A Demons-Based Approach," *Medical Image Computing and Computer-Assisted Intervention - Miccai 2008, Pt I, Proceedings*, 5241, 754-761 (2008).
- [20] D. C. Alexander, C. Pierpaoli, P. J. Basser, and J. C. Gee, "Spatial transformations of diffusion tensor magnetic resonance images," *IEEE Transactions on Medical Imaging*, 20(11), 1131-1139 (2001).
- [21] H. Sundar, D. G. Shen, G. Biros, H. Litt, and C. Davatzikos, "Estimating myocardial fiber orientations by template warping," *2006 3rd Ieee International Symposium on Biomedical Imaging: Macro to Nano, Vols 1-3*, 73-76 (2006).